Adhesion of Polymer Vesicles

John J. Lin,[1] Frank S. Bates,[2] Daniel A. Hammer,[3] and James A. Silas[1,*]

[1]*Department of Chemical and Biomolecular Engineering and the Institute for Medicine and Engineering, University of Pennsylvania, Philadelphia, Pennsylvania, USA*

[2]*Department of Chemical Engineering and Material Science, University of Minnesota, Minneapolis, Minnesota, USA*

[3]*Department of Bioengineering and the Institute for Medicine and Engineering, University of Pennsylvania, Philadelphia, Pennsylvania, USA*

(Received 4 January 2005; published 6 July 2005)

The adhesion and bending modulus of polybutadiene-poly(ethylene oxide) block copolymer vesicles made from a bidisperse mixture of polymers is measured using micropipette aspiration. The adhesion energy between biotinylated vesicles and avidin beads is modeled by incorporating the extension of the adhesive ligands above the surface brush of the vesicle according to the blob model of bidisperse polymer mixtures of Komura and Safran assuming the polymer brush at the surface of the vesicle is compact. The same model accurately reproduces the scaling of the bending modulus with polymer composition.

DOI: 10.1103/PhysRevLett.95.026101 PACS numbers: 68.35.Np, 62.25.+g, 82.35.Gh, 82.70.Uv

Adhesion between polymer brushes and biological surfaces is important in soft condensed materials and biomaterials. The use of polyethylene oxide brushes in medical devices and delivery vehicles is common. Polyethylene oxide has mixed solubility in water [1], and its effect on interfacial properties is not completely understood. In order to understand the relationship between the presence and the presentation of adhesive molecules on a polymer brush for targeted biological adhesion, we have experimentally measured the material and adhesion properties of block copolymer vesicles chemically modified with biotin at their surface. Amphiphilic block copolymers were designed to form vesicles in an aqueous solution where the adhesive surface is the outer self-assembled monolayer of the vesicle bilayer. This surface is analogous to a fluid brush of polymer chains that are anchored in the hydrophobic membrane [2]. The scaling of the fundamental physical properties of fluid polymer brushes has been addressed through self-consistent mean field theories [3–6], Monte Carlo simulations [7,8], and density functional theory [9]. We report the results of adhesion and modulus measurements along with a model based on the physical properties and structure of the adhesive vesicle surface.

Vesicles of polybutadiene-poly(ethylene oxide) (PEO) were made by mixing polymers of different molecular weights, each of which form vesicles on their own: OB2 (3400 Da), OB9 (5000 Da), and OB18 (10 400 Da) [2,10]. The terminal hydroxyl of OB18 is replaced with biotin to form OB18b, which is incorporated into vesicles proportional to its molar concentration in the bulk [11]. Micropipette adhesion measurements were performed by placing similarly sized biotinylated vesicles in contact with a 9.95 μm diameter avidin coated microsphere (Bangs Laboratories, Fisher, Indiana) for 15 min before putting tension on the vesicle to remove it from the surface. This time period allows sufficient time for reproducible contact and adhesion between the fluid brush layer and the solid microsphere. Diffusive strengthening of the contact area is not observed, as the lateral diffusion coefficient of the smallest polymer (OB2) in a bilayer is at least an order of magnitude lower than that for lipids [2].

Adhesion is assessed by the amount of isotropic tension necessary to peel the contact area. A decrease in pressure in the micropipette partially aspirates the fluid vesicle, inducing a tension in the membrane which pulls the vesicle off of the bead. As avidin and biotin release slowly, there is a threshold of force that the contact area will withstand without peeling. The hysteresis displayed in this system is typical of strongly binding interfaces without lateral diffusion, as described by Evans [12]. At a critical tension, T_c, the adhesion contact area peels suddenly and completely. The final pipette pressure and vesicle capsule size are measured after release to calculate the amount of tension that was applied to the vesicle according to [13]

$$T_c = \frac{\Delta P D_p}{4(1 - \frac{D_p}{D_v})}, \tag{1}$$

where ΔP is the pipette pressure, D_p is the diameter of the pipette, and D_v is the diameter of the vesicle capsule. This measurement of tension is more reproducible than an analysis of the geometry present while the vesicle is still attached to the bead. The mechanism of adhesion failure is judged to be separation at the avidin-biotin bond instead of a biotinylated polymer being pulled out of the membrane, as the integrity of the vesicle is maintained and subsequent adhesion measurements with the same vesicle contact area are nearly identical. Similarly sized vesicles and contact areas are used for all samples to minimize the effects of geometry. Theoretically, the amount of tension required to separate the surfaces scales with the adhesive surface energy density, the energy of specific receptor-ligand pairs per area on the surface of the vesicle [12].

The most likely location for a ligand attached to the end of a polymer chain is near the surface of the polymer brush [4,14], which leads to a monotonically increasing critical tension if surface concentration were the only consideration. Figure 1 shows that OB18b mixed with the shortest polymer OB2 gives rise to a maximum in critical tension at intermediate OB18b concentrations that exceed the critical tensions for pure OB18b by a factor of 4. The maximum is less pronounced when OB18b is mixed with OB9 and disappears altogether when OB18b is mixed with unmodified OB18, similar to the results found for the adhesion of functional microbubbles to the surface of PEO modified lipid vesicles [15].

As we observe significant differences between the critical tensions for biotin presented on a monodisperse brush compared with biotin expressed on a bidisperse brush, we incorporate a description of the mechanics of the biotinylated polymer into a structural model of the brush surface. The force necessary to break the adhesion contact is transduced through the polymer chains that connect the two surfaces. When a polymer anchored within the vesicle bilayer and attached to another surface is put under tension, the polymer will stretch out of its equilibrium conformation, which adds an energetic contribution to the bond energy. Some authors report significant energy absorption of PEO chains stretching in water [16]. For simplicity, we approximate the stretching of the polymer from the surface of the brush with a harmonic energy well. We neglect rate dependent terms and model the energy necessary to break the bond as the maximal force needed to separate the bond applied linearly over a bonding distance. The energy of each bond is then simply $\frac{f_{\text{bond}}}{2} l_{\text{bond}}$. This is shown schematically in Fig. 2. The force required to separate a bond is unchanged by the presence of the tether, but the strain required to separate the bond pair is greater as both the polymer chain and bond must be strained simultaneously. Taking the spring constant of the combined bond-polymer pair to be an average, the energy necessary to separate the receptor-ligand bond becomes

$$T_c \propto \frac{\sigma_{\text{bond}}}{A_c}(E_{\text{bond}} + E_{\text{tether}}),$$
$$T_c \propto \frac{\sigma_{\text{bond}}}{A_c}\frac{f_{\text{bond}}}{2}(l_{\text{bond}} + l_{\text{tether}}), \tag{2}$$

where σ_{bond} is the surface density of ligand and A_c is the contact area. The extent of polymer strain, l_{tether}, is the height the polymer may extend above its equilibrium height in the surface brush. We use the results of previous investigations of polymer brushes to evaluate this term.

Many authors have addressed the internal composition of polymers in both mono- and bidisperse brushes [3–5,7,14,17–19]. An exact description of PEO in solution and polymer brushes remains elusive and is a current area of interest [1,5,6,20–23]. In order to understand l_{tether} in light of the complexities attributed to PEO brushes, we use the blob model of Komura and Safran [19] because its results are analytical and predict the scaling of the bending modulus for polymer mixtures (Fig. 3). Within this construction, mixing longer and shorter polymer chains yields a vertically segregated polymer brush where both polymers coexist within the layer closest to the interface, while the longer polymer extends above this layer and forms a second layer (Fig. 2). The results of the model by Komura and Safran differ slightly from numerical self-

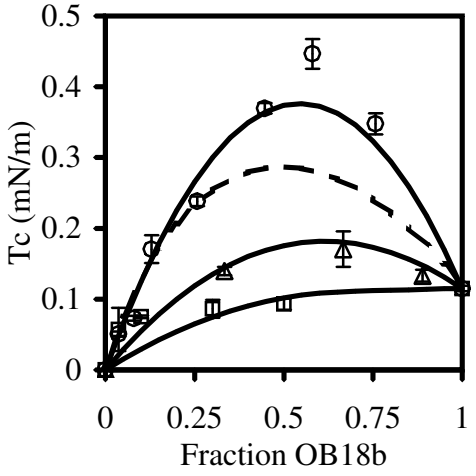

FIG. 1. Plot of the critical tension needed to separate vesicles composed of mixtures of OB18b with OB2 (circles), OB9 (triangles), and OB18 (squares) from an avidin coated microsphere. The two top lines are a comparison of the model [Eq. (5)] with $\nu = \frac{3}{5}$ (dashed line) and $\nu = \frac{1}{3}$ (solid lines) to the data for OB18b in OB2 (circles). The scaling of Eq. (5) ($\nu = \frac{1}{3}$) with the molecular weight of the shorter component (α) is shown with solid lines for the three experimental data sets.

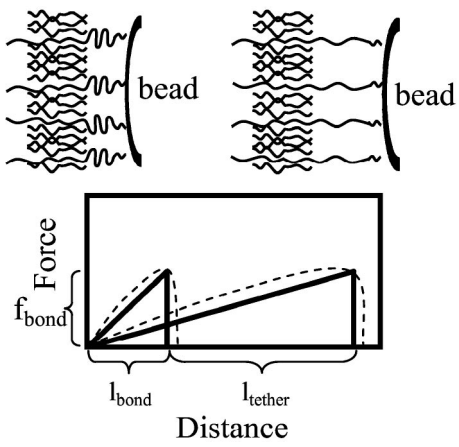

FIG. 2. Diagram of the extension of the polymer tethers away from the surface as tension in applied between the bead and the vesicle. The bonding energy of one functional group is shown schematically with a linear approximation for the bond energy. The same bond expressed on a polymer tether will increase the bond energy (area under the curve) due to the energy required to extend the polymer tether into the solvent.

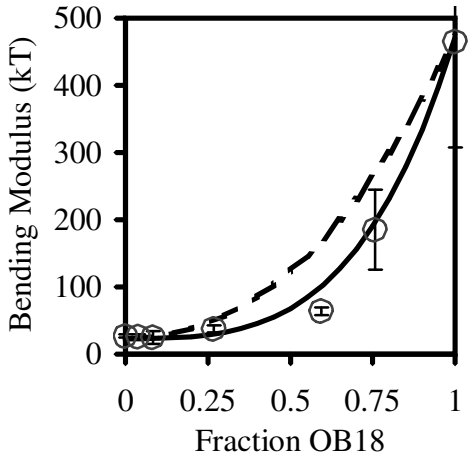

FIG. 3. The bending modulus of mixed OB18/OB2 vesicles as a function of OB18 concentration. Values for fractions of OB18 below 0.6 are measured using a single micropipette, while values above 0.6 are measured using two micropipettes in concert. The dashed line is the scaling from Eq. (6) with $\nu = \frac{3}{5}$, while the solid line is the scaling for $\nu = \frac{1}{3}$. The overall change in the bending modulus between OB18 and OB2 is predicted by the difference in molecular weight, α.

consistent field theory [4], but agree within the experimental error of these measurements.

The height of the unstrained polymer tether is the surface of the polymer brush, and scales with $\alpha h_1 \phi^{(1-\nu)/2\nu}$, where h_1 is the height of a brush made from the shorter polymer,

$$\alpha = \frac{N_L - N_s}{N_s} \tag{3}$$

is the measure of the average molecular weight difference between the longer (N_L) polymer and the shorter (N_s) polymer which compose the membrane, ϕ is molar concentration of the longer polymer in the brush, and ν is the correlation exponent that describes the mean field conformation of the polymer in solvent: the end-to-end distance of the polymer in solvent scales with ν (3/5, 1/2, and 1/3 for a good, theta, and poor solvent, respectively). The maximum extension of the polymer above the surface is the height of the completely stretched brush, αh_1. The choice of exponent is a rough treatment of the conformation of PEO, as it is related to the χ interaction parameter of PEO in water, which changes as a function of temperature and concentration [1,5,6,24]. We treat the correlation exponent only as a description of the overall PEO conformation without reference to solvent quality, as the mean field description is inadequate to describe the interactions of PEO with water. Incorporating these results into Eq. (1) yields

$$T_c \propto \frac{\phi}{A_c} \frac{f_{\text{bond}}}{2} [l_{\text{bond}} + \alpha h_1 (1 - \phi^{(1-\nu)/2\nu})]. \tag{4}$$

Plotting the results for a polymer brush composed of OB18b in OB2 for $\nu = \frac{3}{5}$ or $\frac{1}{3}$ yields the dashed line and the top solid line in Fig. 1, respectively. The value of $\nu = \frac{1}{3}$ most accurately reproduces the details of the experimental data. Physically, this model describes a surface energy density that initially increases as the number of bonding sites increases. However, with each additional OB18b molecule added to the surface, the average height of the polymer brush increases, decreasing the overall extension of every polymer tether and thus the energy of each bond. Through the value of α, Eq. (4) describes how the surface adhesion scales as OB18b is mixed with a base polymer of different molecular weight.

When the functional polymer and the unmodified polymer are similar in length, the physical situation is no longer adequately described by the average tether length above the surface. The polydispersity of OB18b (N_L) is incorporated into α of Eq. (3), yielding a sum of the surface bond energy density over the distribution in tether lengths, P_α. Terms in the sum which yield a negative contribution to the surface energy density are neglected as they correspond to a biotin molecule that is tethered to a short polymer which cannot reach the surface. For the situation of OB18b mixed in OB18, only the longer half of the OB18b molecular weight distribution binds effectively. When the functional polymer is significantly longer than the base membrane, Eq. (4) is recovered, as is the case for OB18b mixed with OB9 and OB2:

$$\begin{aligned} T_c &\propto \sum_\alpha \frac{\sigma_{\text{bond}}(\alpha)}{A_c} E_{\text{bond}}(\alpha), \\ T_c &\propto \sum_\alpha P_\alpha \frac{\phi}{A_c} \frac{f_{\text{bond}}}{2} [l_{\text{bond}} + \alpha h_1 (1 - \phi^{(1-\nu)/2\nu})]. \end{aligned} \tag{5}$$

Equation (5) is shown as the solid lines in Fig. 1 using the reported molecular weight distribution for OB18. Other considerations such as ligand availability or substrate deformability may also play a role in the adhesion of polymer vesicles, but a mechanical description of the polydispersity of the polymer tethers above the average height of the brush is sufficient to reproduce the results shown here.

The brush architecture described in the paper of Komura and Safran provides a prediction for the bending modulus of mixed polymer layers as a function of their molecular weight difference, concentration, and correlation exponent. While the area expansion, shear, and bending modulus for pure OB2 and OB18 have been reported previously [25], we report the bending modulus of mixed polymer vesicles measured with micropipette aspiration. For bending moduli below 50 kT, a single pipette technique is used to measure the tension-strain curve for unilamellar vesicles. At low strains, there is a logarithmic regime due to vesicle undulations that is used to measure the bending modulus [13]. For stiffer membranes, the logarithmic regime is too small to measure accurately, so a dual-pipette technique is

utilized where the minimum tension to deform prestressed vesicles is measured [26].

As shown in Fig. 3, as OB18 is added to the polymer brush the bending modulus remains constant around the value for pure OB2. The bending modulus of the mixture increases significantly only after the longer polymer becomes the majority component. OB18 mixing with OB2 is essentially the case described in Fig. 6(a) of Ref. [19], which gives a scaling of

$$\frac{k_{\mathrm{mix}}}{k_{\mathrm{OB2}}}(\alpha, \phi, \nu) = 1 + 3\alpha\phi^{(1+2\nu)/2\nu} + 3\alpha^2\phi^{(2+\nu)/2\nu} + \alpha^3\phi^{3/2\nu}. \quad (6)$$

This equation predicts the change in the bending modulus with a concentration and molecular weight difference of the polymer mixture given the value of the bending modulus for OB2, as shown in Fig. 3. The value of the bending modulus of pure OB18 bilayers ($\phi = 1$) is recovered using the molecular weight difference between OB2 and OB18. Intermediate values are best reproduced using $\nu = \frac{1}{3}$, in agreement with our adhesion measurements.

A value of $\nu = \frac{1}{3}$ is adequate to reproduce both the adhesion and bending modulus data, indicating that at least part of the PEO bilayer scales as a compact polymer brush at the surface. While the complex issue of PEO conformation cannot be described with a single correlation exponent, these measurements indicate a more compact layer at the surface than one would expect for a polymer in good solvent. These results are consistent with other investigations of PEO that indicate a more compact state, including atomic force microscopy measurements consistent with specific hydrogen bonding that cross-links polymer segments [16], an increased concentration of PEO near the bilayer interface detected with small angle neutron scattering [27], and thermodynamic models for a two-state conformational transition with concentration that influences PEO's hydrophobicity [1,5].

This work indicates that the strength of the receptor-ligand bond is only one factor in the development of biologically adhesive surfaces, and the strength of adhesion may be engineered with how those bonds are presented at the surface. By varying the presentation of different biological ligands, the specific surface adhesivity may be modulated. This also indicates that the structure of the surface must be taken into account to model the adhesion of polymer brushes, and that interfacial adhesivity can be used to interrogate interfacial structures.

The authors gratefully acknowledge the funding from PENN MRSEC, Minnesota MRSEC, NASA Materials Science, and NIH EB003457. J. J. L. acknowledges support from the NASA Graduate Student Researchers Program (GSRP). J. A. S. acknowledges funding from the National Institutes of Health under Ruth L. Kirschstein National Research Service Grant No. 1 F32 GM068297-01 from the National Institute of General Medical Sciences.

*Current address: Department of Chemical Engineering, Texas A&M University, College Station, TX, USA.

[1] G. Karlstrom, J. Phys. Chem. **89**, 4962 (1985).
[2] B. M. Discher, Y. Y. Won, D. S. Ege, J. C. Lee, F. S. Bates, D. E. Discher, and D. A. Hammer, Science **284**, 1143 (1999).
[3] F. A. M. Leermakers, C. M. Wijmans, and G. J. Fleer, Macromolecules **28**, 3434 (1995).
[4] N. Dan and M. Tirrell, Macromolecules **26**, 6467 (1993).
[5] V. A. Baulin, E. B. Zhulina, and A. Halperin, J. Chem. Phys. **119**, 10 977 (2003).
[6] V. A. Baulin and A. Halperin, Macromol. Theory Simul. **12**, 549 (2003).
[7] M. P. Pepin and M. D. Whitmore, J. Chem. Phys. **114**, 8181 (2001).
[8] S. Rex, M. J. Zuckermann, M. Lafleur, and J. R. Silvius, Biophys. J. **75**, 2900 (1998).
[9] S. D. Stoyanov, V. N. Paunov, H. Kuhn, and H. Rehage, Macromolecules **36**, 5032 (2003).
[10] J. C. Lee, H. Bermudez, B. M. Discher, M. A. Sheehan, Y. Y. Won, F. S. Bates, and D. E. Discher, Biotechnol. Bioeng. **73**, 135 (2001).
[11] J. J. Lin, J. A. Silas, H. Bermudez, V. T. Milam, F. S. Bates, and D. A. Hammer, Langmuir **20**, 5493 (2004).
[12] E. A. Evans, Biophys. J. **48**, 185 (1985).
[13] E. Evans and W. Rawicz, Phys. Rev. Lett. **64**, 2094 (1990).
[14] A. M. Skvortsov, L. I. Klushin, and A. A. Gorbunov, Macromolecules **30**, 1818 (1997).
[15] D. H. Kim, A. L. Klibanov, and D. Needham, Langmuir **16**, 2808 (2000).
[16] F. Oesterhelt, M. Rief, and H. E. Gaub, New J. Phys. **1**, 6 (1999).
[17] P. Auroy, L. Auvray, and L. Leger, Phys. Rev. Lett. **66**, 719 (1991).
[18] M. P. Pepin and M. D. Whitmore, Macromolecules **33**, 8644 (2000).
[19] S. Komura and S. A. Safran, Eur. Phys. J. E **5**, 337 (2001).
[20] D. L. Ho, B. Hammouda, and S. R. Kline, J. Polym. Sci., B, Polym. Phys. **41**, 135 (2003).
[21] S. R. Sheth and D. Leckband, Proc. Natl. Acad. Sci. U.S.A. **94**, 8399 (1997).
[22] E. P. K. Currie, M. Wagemaker, M. A. C. Stuart, and A. A. van Well, Macromolecules **32**, 9041 (1999).
[23] E. P. K. Currie, F. A. M. Leermakers, M. A. C. Stuart, and G. J. Fleer, Macromolecules **32**, 487 (1999).
[24] V. A. Baulin and A. Halperin, Macromolecules **35**, 6432 (2002).
[25] H. Bermudez, D. A. Hammer, and D. E. Discher, Langmuir **20**, 540 (2004).
[26] D. V. Zhelev, D. Needham, and R. M. Hochmuth, Biophys. J. **67**, 720 (1994).
[27] Y. Y. Won, H. T. Davis, F. S. Bates, M. Agamalian, and G. D. Wignall, J. Phys. Chem. B **104**, 7134 (2000).